Electronic Supplementary Material (ESI) for Nanoscale.

Supporting Information

Near-Field Asymmetries in Plasmonic Resonators

*Vladimir Aksyuk, Basudev Lahiri, Glenn Holland, and Andrea Centrone**

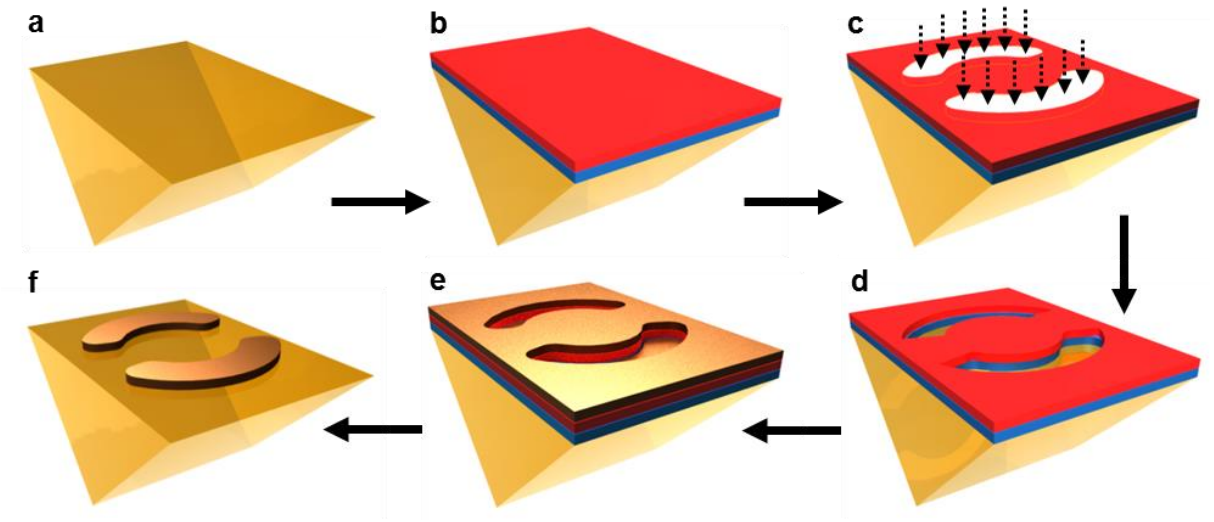

Figure S1. Nanofabrication scheme: a) A ZnSe right angle prism is used as a substrate for the ASRRs fabrication, b) a poly(methyl methacrylate) (PMMA) bilayer (250 nm and 350 nm) was spun on the ZnSe prism, c) the ASRRs arrays were written with electron beam lithography, d) the pattern is developed with Methyl Iso-butylketone and isopropyl alcohol e) a 5 nm chromium adhesion layer and a 150 nm gold layer is deposited with electron beam deposition, f) The ASRRs arrays are obtained after lift of in hot acetone.

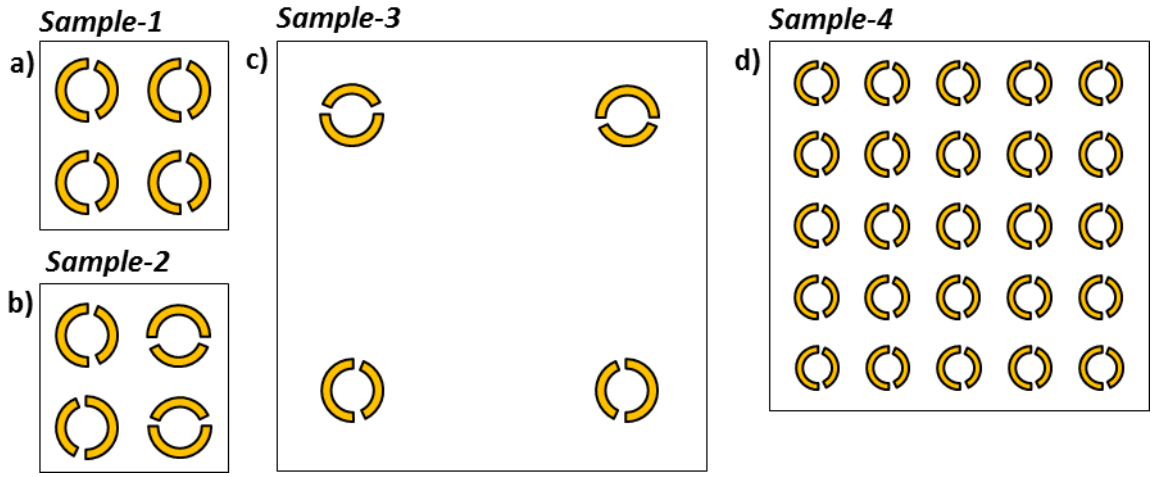

Figure S2. Schematic description of the ASRR arrays: a) Sample-1 consist of an ASRRs square array made by resonators with 1.9 µm diameter, all with the same orientation and pitch with respect to the nearest neighbor of 3.0 µm ± 0.1 µm. b) Sample-2 consists of an ASRRs square array made by a unit cell with 4 resonators with four different orientations, each with 2.0 µm diameter and pitch of 3.0 µm ± 0.1 µm. c) Sample-3 has unit cell with 4 resonators with 4 different orientations, rotated by 90° anticlockwise with respect to sample-2 and has a pitch of 10.0 µm. d) sample-4 is made by a 5x5 square array made by ASRRs with the same orientation with a diameter 1.4 µm and pitch of 2.0 µm.

Supplemental discussion 1

In a dense periodic array the individual plasmonic resonances can couple and form bands, resulting in enhanced coherent excitation under appropriate energy and phase matching with incident radiation, the so-called array effect.[1-3] This effect was assessed by measuring a small square array (5 x 5 resonators) with very closed packed resonators all with the same orientation (*Sample-4, figure S2d*) diameter 1.4 µm ± 0.1 µm and pitch of 2.0 µm ± 0.1 µm all with the same orientation . The PTIR image on this sample (figure S3) shows the intensity of the near-field hot spots (enhancement) increases from left to right across the small array suggesting that the near-field coupling between neighboring resonators results in unidirectional energy build up in the array. In fact the weaker hot-spots at top and bottom of the array that are generated by single ASRR (vs. two ASRRs for all others) also have the same left to right buildup.

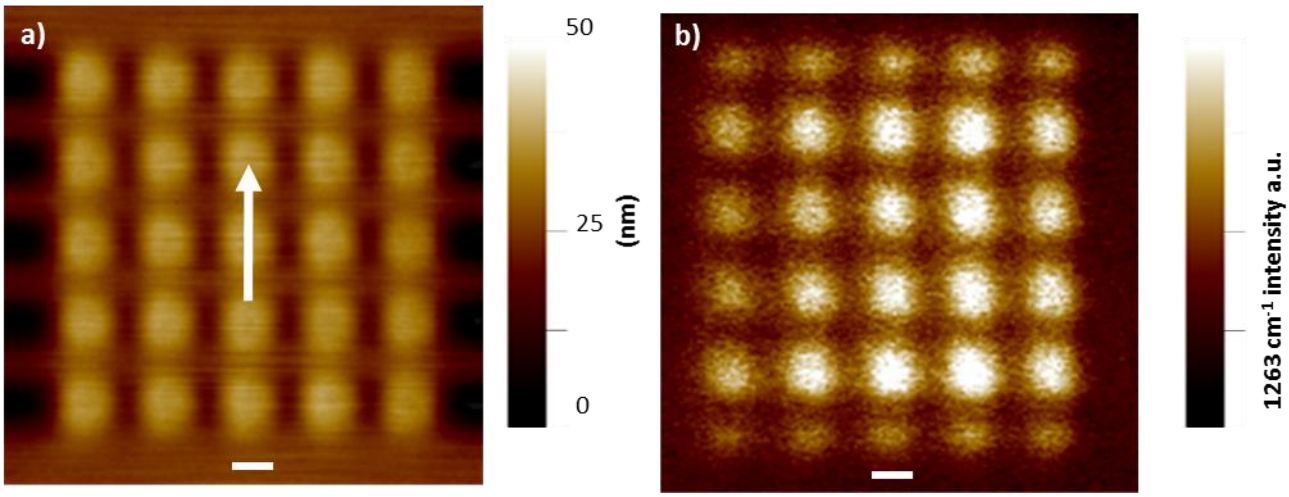

Figure S3. a) AFM height image of *sample-4* coated with a 200 nm PMMA film; the white arrow indicates the direction of the electric field polarization in the PTIR image. b) Corresponding PTIR image of the PMMA C-O stretching vibrational mode at 1263 cm^{-1} (7.92 µm). Because the light is preferentially scattered in the right direction the intensity of the near-field hot spots increases approximately 3-fold from left to right. Scale bars are 1.0 µm.

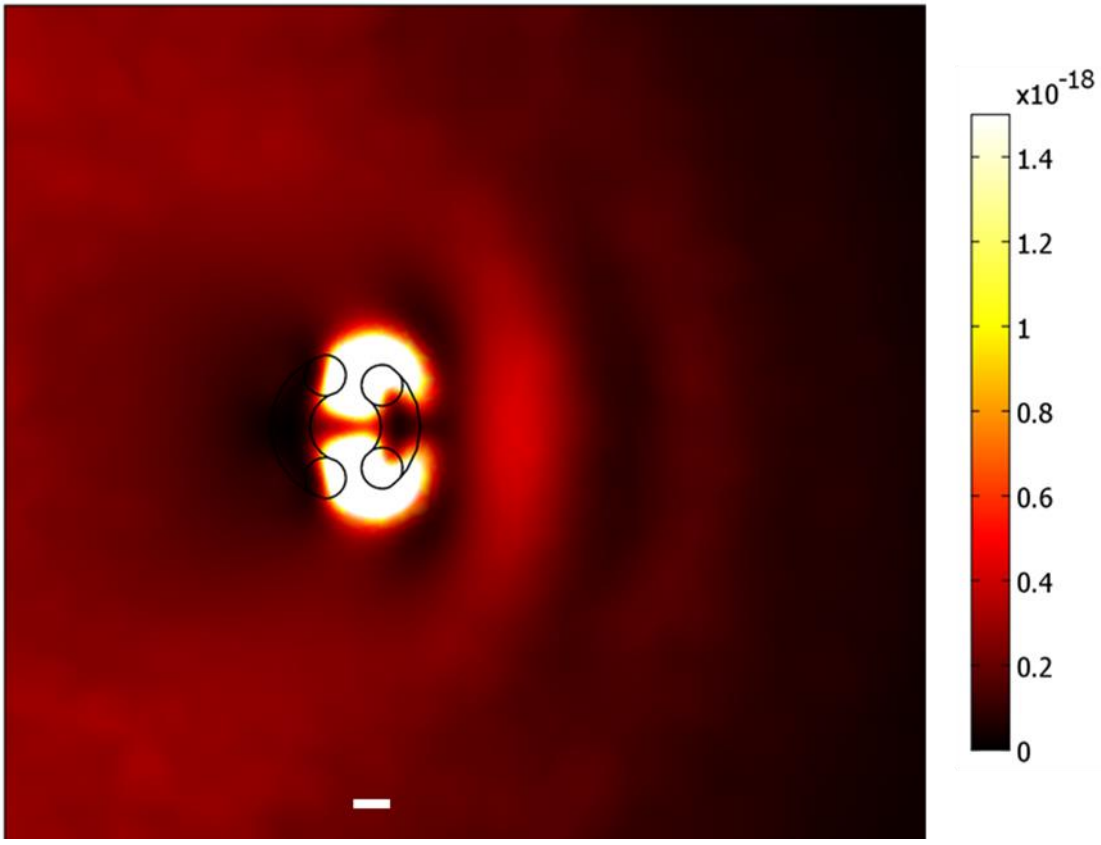

Figure S4. Numerical simulation results, obtained when illuminating the structure with s-polarized 1191 cm^{-1} (8.4 µm) light at + 45° with parallel polarization, same as in figure 4c, except different view area and vertical scale are used to illustrate the interference pattern resulting from the resonators directional scattering. The figure shows the energy density in PMMA integrated along the film thickness (z) and convolved with a 200 nm waste Gaussian peak function (similar to the film thickness) to approximately account for the thermal and mechanical effects of the PTIR experiment. Scale bars is 500 nm.

Supplemental discussion 2

Based on the simulations, the distribution of hot-spots for perpendicular polarization (figure 4d of the main text) is the result of superposition of both electrical and magnetic excitation in the resonators. Specifically, the resonator response is the superposition of (1) a magnetically excited antisymmetric dark mode and (2) the electrical polarization induced in the metal along the applied electric field, (perpendicular to the arcs, in the resonator plane).

The electric fields in the two gaps have opposite directions for (1) and the same direction for (2). Therefore these contributions add constructively in one of the gaps and destructively in the other, suppressing one of the gap hotspots. The regions of field enhancement outside the arc centers originate from (2), but are shifted from the ASRR's symmetry plane by the addition of (1).

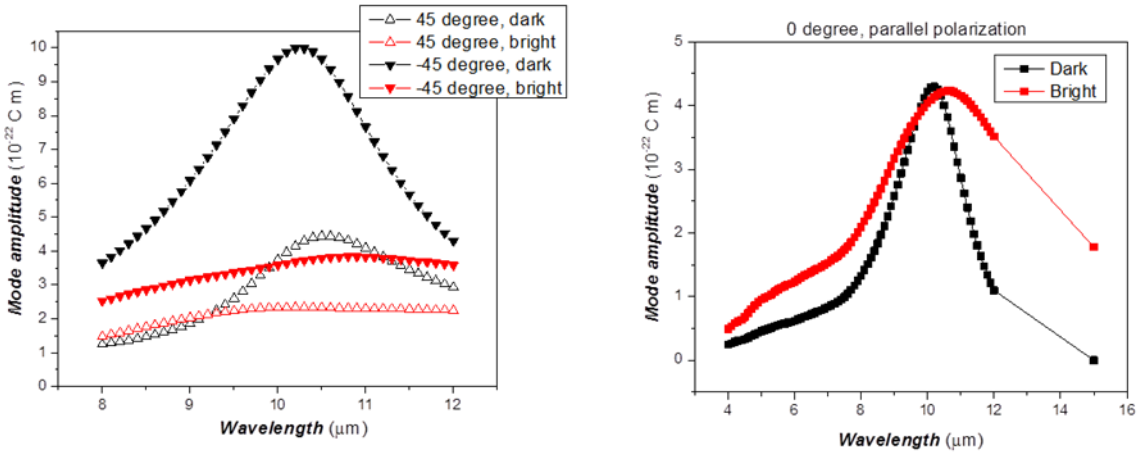

Figure S5. Numerically calculated spectra of dark and bright modes excited at plus and minus 45° (a) and 0° (b) with s-polarized light with polarization parallel to the arcs incident from the ZnSe side.

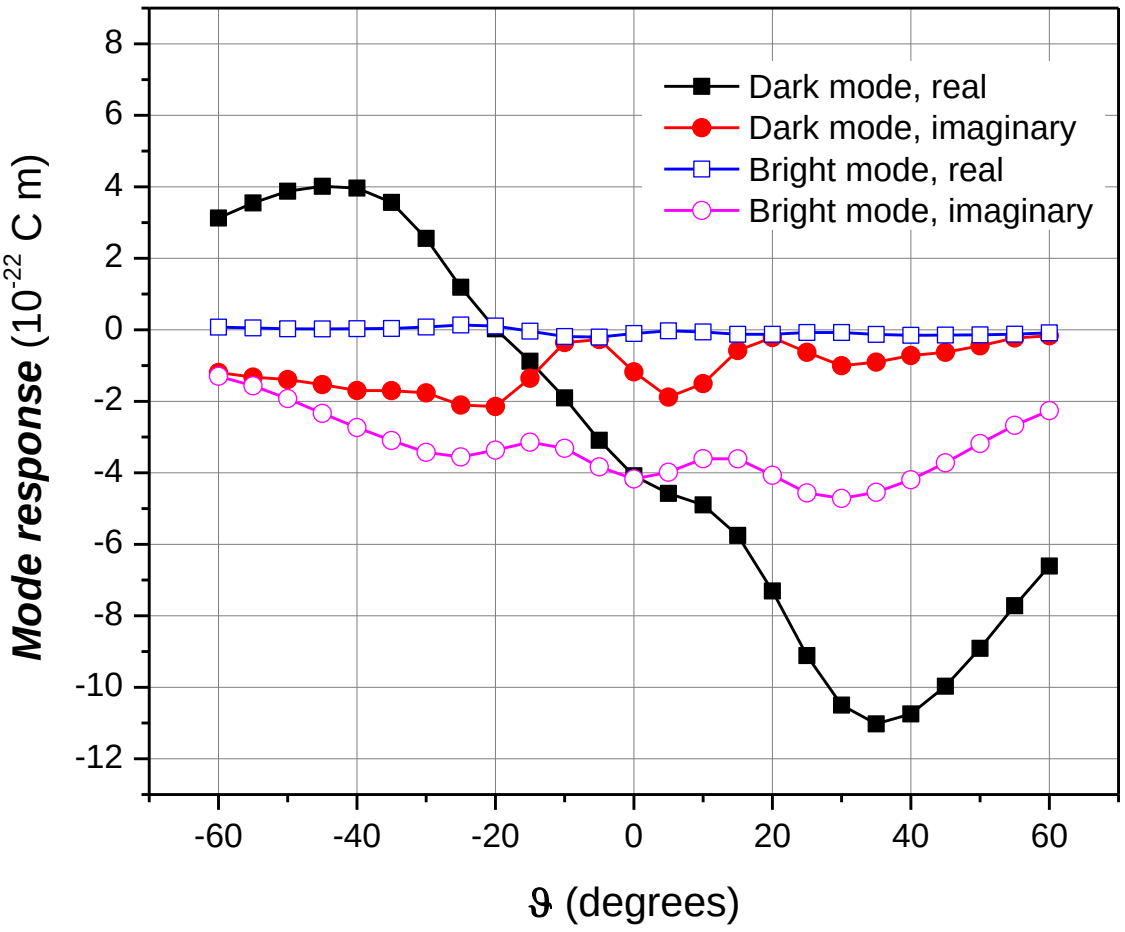

Figure S6. Values of the bright and dark mode complex responses at of 971 cm^{-1} (10.3 μm) as a function of the incident angle ϑ (Same as Figure 5c, but with both dark and bright mode responses shown).

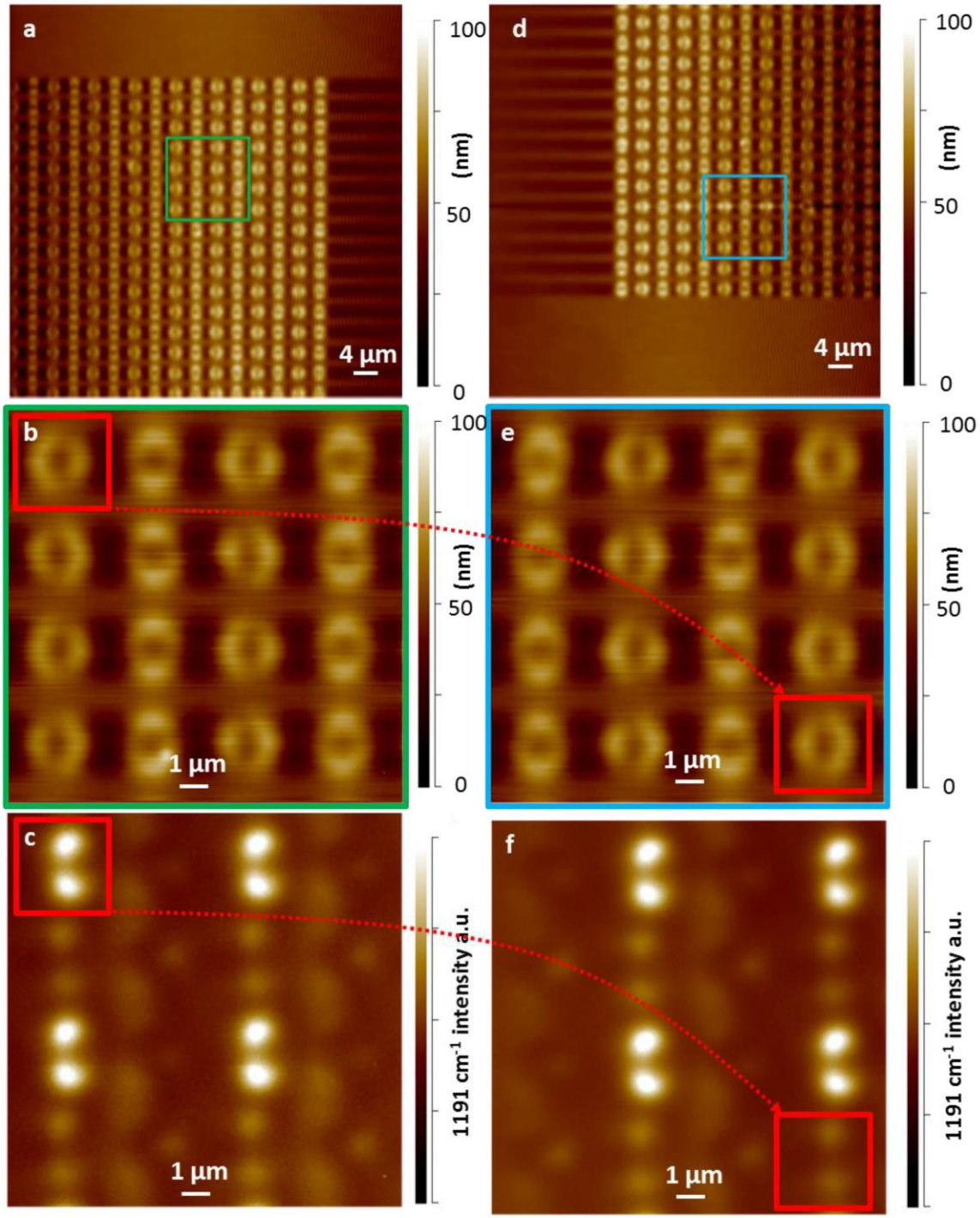

Figure S7. a) Large area AFM height image of sample-2 coated with a 200 nm PMMA film. b) AFM height image of sample-2 corresponding to the resonators included in the green square box in panel a. c) PTIR image of the PMMA CH_3 wagging mode at 1191 cm-1 (8.40 µm) showing near-field SEIRA hot spots in the PMMA layer for the resonators included in the green square box in panel a. d) Large area AFM height image of sample-2 obtained by rotating the prism by 180°. e) AFM height image of sample-2 corresponding to the resonators included in the blue square box in panel d obtained by rotating the prism 180°. f) PTIR image of the PMMA CH_3 wagging mode at 1191 cm-1 (8.40 µm) showing near-field SEIRA hot spots in the PMMA layer for the resonators included in the blue square box in panel d, obtained by rotating the prism by 180°. The red square boxes highlight the response of a particular resonator. The hot-spot intensity of the resonators illuminated for parallel polarization switch from intense to weak and vice versa by rotating the prism by 180 degrees.

Supplemental references

1. R. Adato, A. A. Yanik, J. J. Amsden, D. L. Kaplan, F. G. Omenetto, M. K. Hong, S. Erramilli and H. Altug, *Proc. Natl. Acad. Sci. U. S. A.*, 2009, **106**, 19227-19232.
2. N. Papasimakis, V. A. Fedotov, Y. H. Fu, D. P. Tsai and N. I. Zheludev, *Phys. Rev. B*, 2009, **80**, 041102.
3. C. H. Wu, A. B. Khanikaev, R. Adato, N. Arju, A. A. Yanik, H. Altug and G. Shvets, *Nat. Mater.*, 2012, **11**, 69-75.